

# The c-quark EDM and production of $h_c$ in $e^+e^-$ annihilation

Xiao-Jun Bi<sup>a</sup>, Tai-Fu Feng<sup>b</sup>, Xue-Qian Li<sup>c</sup>, Jukka Maalampi<sup>b</sup>, Xinmin Zhang<sup>d</sup>

<sup>a</sup>*Key Laboratory of Particle Physics, Institute of High Energy Physics,*

*Chinese Academy of Sciences, P.O. Box 918-3,*

*Beijing 100049, People's Republic of China*

<sup>b</sup>*Department of Physics, 40014 University of Jyväskylä, Finland*

<sup>c</sup>*Department of Physics, Nankai University, Tianjing 300071, P. R. China*

<sup>d</sup>*Theoretical Physics Division, Institute of High Energy Physics,*

*Chinese Academy of Sciences, P.O. Box 918-4,*

*Beijing 100049, People's Republic of China*

(Dated: May 25, 2018)

## Abstract

We analyze the charm quark electric dipole moment (EDM) in the minimal supersymmetric extension of the standard model (MSSM), including important two-loop gluino contributions. Considering the experimental constraint on the neutron EDM, the theoretical prediction for the charm quark EDM can reach about  $10^{-20} e \cdot cm$ . If taking into account the mixing between the scharm and stop quarks in the effective supersymmetry scenario, the charm quark EDM can be enhanced to  $\sim 10^{-19} e \cdot cm$ . Direct production of the CP-odd  $^1P_1$  state  $h_c$  in  $e^+e^-$  annihilation via the CP-violating process at the BES-III and CLEO-C is analyzed.

PACS numbers: 11.30.Er, 12.60.Jv, 14.80.Cp

Keywords: electric dipole moment, charm quark, supersymmetry

## I. INTRODUCTION

Up to now, CP violation is only found in the  $K$ -[1] and  $B$ -system[2], which can be well explained within the standard model (SM) of electroweak interaction. As is well known, electric dipole moment (EDM) of an elementary particle is a clear signature of CP violation. However, EDM of a fermion does not appear up to two-loop order, and the three-loop contributions partially cancel among each others in the SM. Therefore, observation of sizable EDM of an elementary fermion would definitely be a signal of existence of new physics beyond the SM with extra CP phases.

Supersymmetry (SUSY) is now believed to be the most attractive scenario for new physics. Beside the Cabibbo-Kobayashi-Maskawa (CKM) mechanism, the soft breaking terms provide a new source of  $CP$  and flavor violation in the minimal supersymmetric extension of the standard model (MSSM). Those  $CP$  violating phases can affect some important observables in the mixing of Higgs bosons [3], the lepton and neutron electric dipole moments (EDMs) [4, 5], lepton polarization asymmetries in the semi-leptonic decays [6], the production of  $P$ -wave charmonium and bottomonium [7], and  $CP$  violation in rare  $B$ -decays and  $B^0\bar{B}^0$  mixing [8]. At present, the strictest constraints on those  $CP$  violation phases originate from the lepton and neutron EDMs. Since the lepton and neutron EDMs have not been measured so far, there are several suggestions to keep the theoretical estimate of the neutron and electron EDMs below the experimental limits, they are (i) choosing small CP phases  $\lesssim \mathcal{O}(10^{-3})$ [9], (ii) finding appropriate parameter domain where various contributions cancel with each other[10], or (iii) making the first two generations of scalar fermions heavy enough (heavier than 20 TeV) while keeping the soft masses of the third generation below TeV to keep the Higgs boson naturally light[11].

In this work we calculate the charm quark EDM in the  $CP$  violating MSSM. As pointed out in [4], the quark chromoelectric dipole moment (CEDM) makes important contributions to the quark EDM at a low energy scale. In addition, there is a parameter space where some two-loop gluino diagrams provide important contributions to the quark EDM. In our analysis, we include all the contributions from those pieces. We first work in the simplest model, neglecting the new possible flavor violation sources except the CKM mechanism, and avoiding any assumptions about unification of the soft breaking parameters. We find that the charm EDM can reach about  $10^{-20}e \cdot cm$ . Then we also calculate the charm quark

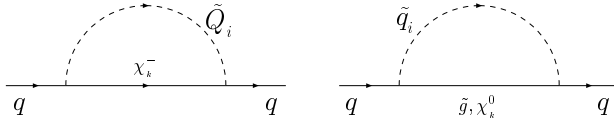


FIG. 1: The one-loop self energy diagrams which lead to quark EDM and CEDM in the MSSM, the corresponding triangle diagrams are obtained by attaching a photon or gluon line to the self-energy blob in all possible ways.

EDM in the effective supersymmetry scenario[16] where the scenario (iii) mentioned above is accommodated. Since the first two-generation sfermions are very heavy, the charm quark EDM is greatly suppressed in this scenario. However, while considering large mixing between the second and the third generation sfermions we find that the charm quark EDM can be greatly enhanced to as large as about  $10^{-19}e \cdot cm$ . The reason is that, since the effective operator which determines the charm quark EDM induces a chiral flip, the large mixing between the scharm and stop can enhance the charm quark EDM due to the top quark mass.

The analysis in Refs. [17, 18] shows that the EDM of heavy quark plays an important role in the direct production of singlet P-wave quarkonia, thus with upgraded BEPC[19] and CLEO-C programs[20], it might be possible to produce the  $^1P_1$  charmonium state,  $h_c$ , directly. Conversely, if no  $h_c$  meson is observed, an upper bound on the charm quark EDM would be set.

The paper is organized as follows: In the next section, we give the analytic expressions of the charm quark EDM and CEDM in  $CP$  violating MSSM. In Section III we present the numerical results. Section IV is devoted to discuss  $h_c$  production which is closely associated with the magnitude of the charm quark EDM, at  $e^+e^-$  colliders. Finally we conclude in section V.

## II. THE CHARM QUARK EDM

In the effective Lagrangian, the charm quark EDM is defined through a dimension-five operator

$$\mathcal{L}_{EDM} = -\frac{i}{2}d_c\bar{c}\sigma^{\mu\nu}\gamma_5 c F_{\mu\nu} \quad (1)$$

with  $F_{\mu\nu}$  being the electromagnetic field strength. In a theoretical framework with  $CP$  violation, the corresponding loop diagrams induce the charm EDMs. Since quarks also take part in the strong interaction, the chromoelectric dipole moment (CEDM) operator is

$$\bar{c}T^a\sigma^{\mu\nu}\gamma_5 c G_{\mu\nu}^a,$$

where  $T^a$  ( $a = 1, \dots, 8$ ) denote the generators of the strong  $SU(3)$  gauge group and  $G_{\mu\nu}^a$  is the chromo-electromagnetic field strength. This operator contributes to  $d_c$  at low energy scale. In principle, the dimension-six Weinberg operator and two-loop Bar-Zee diagrams all provide contributions to  $d_c$ . Nevertheless, the contributions from the Weinberg operator and Bar-Zee diagrams to  $d_c$  can be ignored safely as we consider the constraint on the neutron EDM. The best way to describe certain loop-induced contributions is the effective theory approach, where the heavy particles are integrated out at the matching scale and the effective theory includes a full set of  $CP$  violating operators. In this work, we restrict ourselves to the following operators that are relevant to the c-quark EDM

$$\mathcal{L}_{eff} = -\frac{i}{2}d_c^{\gamma}\bar{c}\sigma^{\mu\nu}\gamma_5 c F_{\mu\nu} - \frac{i}{2}d_c^g\bar{c}T^a\sigma^{\mu\nu}\gamma_5 c G_{\mu\nu}^a. \quad (2)$$

The one-loop supersymmetric contributions to the Wilson coefficients in Eq. (2) originate from three types of graphs: gluino-squark, chargino-squark, and neutralino-squark loops (FIG.1). Details about the descriptions are presented in ref.[13]. The contributions of the one-loop gluino-squark diagrams are

$$\begin{aligned} d_{\tilde{g}(1)}^{\gamma} &= -\frac{2}{3\pi}e_u e\alpha_s \sum_{i=1}^2 \text{Im}\left((\mathcal{Z}_{\tilde{c}})_{2,i}(\mathcal{Z}_{\tilde{c}}^{\dagger})_{i,1}e^{-i\theta_3}\right) \\ &\quad \times \frac{|m_{\tilde{g}}|}{m_{\tilde{c}_i}^2} B\left(\frac{|m_{\tilde{g}}|^2}{m_{\tilde{c}_i}^2}\right), \\ d_{\tilde{g}(1)}^g &= \frac{g_3\alpha_s}{4\pi} \sum_{i=1}^2 \text{Im}\left((\mathcal{Z}_{\tilde{c}})_{2,i}(\mathcal{Z}_{\tilde{c}}^{\dagger})_{i,1}e^{-i\theta_3}\right) \\ &\quad \times \frac{|m_{\tilde{g}}|}{m_{\tilde{c}_i}^2} C\left(\frac{|m_{\tilde{g}}|^2}{m_{\tilde{c}_i}^2}\right). \end{aligned} \quad (3)$$

Here  $\alpha = e^2/(4\pi)$ ,  $\theta_3$  denotes the phase of  $m_{\tilde{g}}$ , and  $\mathcal{Z}_{\tilde{q}}$  ( $q = u, \dots, b$ ) are the mixing matrices of squarks, i.e.  $\mathcal{Z}_{\tilde{q}}^\dagger \mathbf{m}_{\tilde{q}}^2 \mathcal{Z}_{\tilde{q}} = \text{diag}(m_{\tilde{q}_1}^2, m_{\tilde{q}_2}^2)$  where

$$\mathbf{m}_{\tilde{q}}^2 = \begin{pmatrix} m_{\tilde{Q}}^2 + m_q^2 + m_z^2(\frac{1}{2} - Q_q s_w^2) \cos 2\beta & m_q(A_q^* - \mu R_q) \\ m_q(A_q - \mu^* R_q) & m_{\{\tilde{U}, \tilde{D}\}}^2 + m_q^2 + m_z^2(\frac{1}{2} - Q_q s_w^2) \cos 2\beta \end{pmatrix}, \quad (4)$$

with  $Q_q = 2/3(-1/3)$ ,  $R_q = \tan \beta(1/\tan \beta)$  for  $q = u (d)$ .  $\tan \beta = \frac{v_u}{v_d}$  is the ratio between the up- and down-type Higgs vacua, and  $\theta_w$  is the Weinberg angle. The shortened notations  $s_w = \sin \theta_w$ ,  $c_w = \cos \theta_w$  are adopted. The loop functions are

$$B(r) = [2(r-1)^2]^{-1}[1+r+2r \ln r/(r-1)], \quad C(r) = [6(r-1)^2]^{-1}[10r-26-(2r-18) \ln r/(r-1)].$$

In a similar way, the one loop neutralino-squark contributions can be written as

$$\begin{aligned} d_{\chi_k^0(1)}^\gamma &= e_u \frac{e\alpha}{16\pi s_w^2 c_w^2} \sum_{i,k} \text{Im} \left( (A_N^c)_{k,i} (B_N^c)_{i,k}^\dagger \right) \\ &\quad \times \frac{m_{\chi_0^k}}{m_{\tilde{c}_i}^2} B \left( \frac{m_{\chi_0^k}^2}{m_{\tilde{c}_i}^2} \right), \\ d_{\chi_k^0(1)}^g &= \frac{g_3 \alpha_s}{64\pi s_w^2 c_w^2} \sum_{i,k} \text{Im} \left( (A_N^c)_{k,i} (B_N^c)_{i,k}^\dagger \right) \\ &\quad \times \frac{m_{\chi_0^k}}{m_{\tilde{c}_i}^2} B \left( \frac{m_{\chi_0^k}^2}{m_{\tilde{c}_i}^2} \right) \end{aligned} \quad (5)$$

with

$$\begin{aligned} (A_N^c)_{k,i} &= -\frac{4}{3} s_w (\mathcal{Z}_{\tilde{c}})_{2,i} (\mathcal{Z}_N)_{1,k} + \frac{m_c c_w}{m_w s_\beta} \\ &\quad \times (\mathcal{Z}_{\tilde{c}})_{1,i} (\mathcal{Z}_N)_{4,k}, \\ (B_N^c)_{k,i} &= (\mathcal{Z}_{\tilde{c}})_{1,i} \left( \frac{s_w}{3} (\mathcal{Z}_N)_{1,k}^* + c_w (\mathcal{Z}_N)_{2,k}^* \right) \\ &\quad + \frac{m_c c_w}{m_w s_\beta} (\mathcal{Z}_{\tilde{c}})_{2,i} (\mathcal{Z}_N)_{4,k}^*. \end{aligned} \quad (6)$$

Here  $\alpha_s = g_3^2/(4\pi)$ ,  $s_\beta = \sin \beta$ ,  $c_\beta = \cos \beta$ , and  $\mathcal{Z}_N$  is the mixing matrix of neutralinos.

Finally, the chargino-squark contributions are formulated as

$$\begin{aligned}
d_{x_k^\pm(1)}^\gamma &= \frac{e\alpha}{4\pi s_w^2} V_{cQ}^\dagger V_{Qc} \sum_{i,k} \text{Im} \left( (A_C^Q)_{k,i} (B_C^Q)_{i,k}^\dagger \right) \frac{m_{x_k^\pm}}{m_{\tilde{Q}_i}^2} \\
&\quad \times \left[ e_d B \left( \frac{m_{x_k^\pm}^2}{m_{\tilde{Q}_i}^2} \right) + (e_u - e_d) A \left( \frac{m_{x_k^\pm}^2}{m_{\tilde{Q}_i}^2} \right) \right], \\
d_{x_k^\pm(1)}^g &= \frac{g_3\alpha}{4\pi s_w^2} V_{cQ}^\dagger V_{Qc} \sum_{i,k} \text{Im} \left( (A_C^Q)_{k,i} (B_C^Q)_{i,k}^\dagger \right) \\
&\quad \times \frac{m_{x_k^\pm}}{m_{\tilde{Q}_i}^2} B \left( \frac{m_{x_k^\pm}^2}{m_{\tilde{Q}_i}^2} \right)
\end{aligned} \tag{7}$$

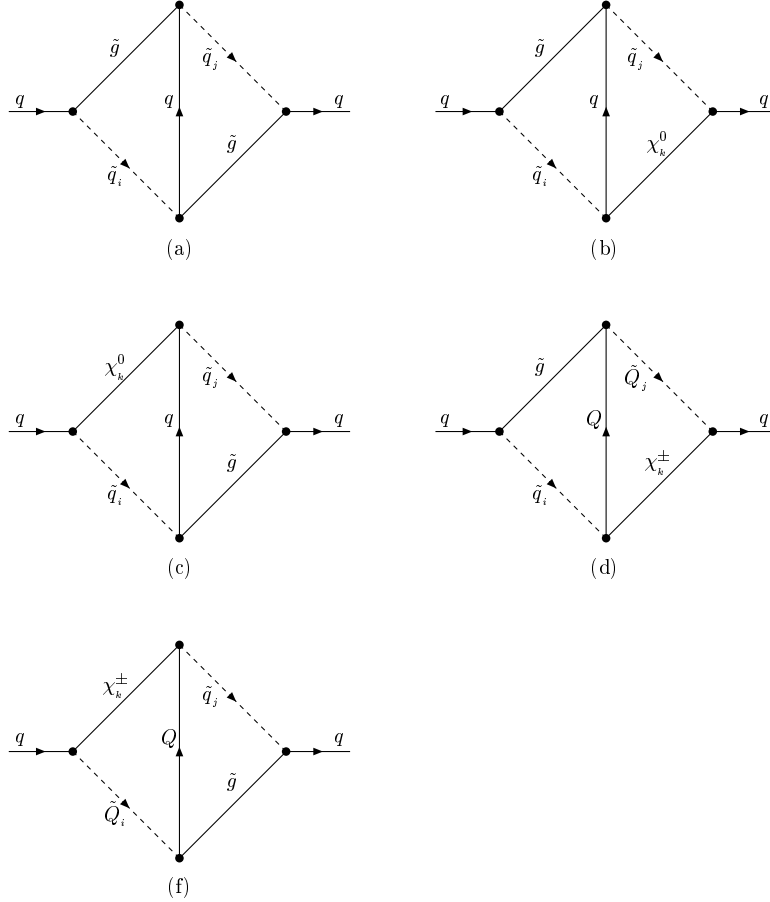


FIG. 2: The two-loop self energy diagrams which lead to quark ( $q = u$  ( $d$ ),  $Q = d$  ( $u$ )) EDM and CEDM in the MSSM, the corresponding triangle diagrams are obtained by attaching an external photon or gluon line to the self-energy diagrams in all possible ways.

where  $V$  denotes the CKM matrix, and the loop function is

$$A(r) = 2(1-r)^{-2}[3-r+2\ln r/(1-r)].$$

The couplings are defined as

$$\begin{aligned} (A_C^d)_{k,i} &= \frac{m_u}{\sqrt{2}m_w s_\beta} (\mathcal{Z}_{\bar{d}})_{1,i} (\mathcal{Z}_+)_{2,k}, \\ (B_C^d)_{k,i} &= \frac{m_d}{\sqrt{2}m_w c_\beta} (\mathcal{Z}_{\bar{d}})_{2,i} (\mathcal{Z}_-)_{2,k} - (\mathcal{Z}_{\bar{d}})_{1,i} (\mathcal{Z}_-)_{1,k}, \\ (A_C^u)_{k,i} &= \frac{m_d}{\sqrt{2}m_w c_\beta} (\mathcal{Z}_{\bar{u}})_{1,i} (\mathcal{Z}_-)_{2,k}^*, \\ (B_C^u)_{k,i} &= \frac{m_u}{\sqrt{2}m_w s_\beta} (\mathcal{Z}_{\bar{u}})_{2,i} (\mathcal{Z}_+)_{2,k}^* - (\mathcal{Z}_{\bar{u}})_{1,i} (\mathcal{Z}_+)_{1,k}^*, \end{aligned} \quad (8)$$

where  $\mathcal{Z}_\pm$  are the right- and left-handed mixing matrices of the charginos. Noting that one-loop chargino contributions to the quark EDMs and CEDMs are proportional to a suppression factor  $\frac{m_q}{m_w}$  which exists in all the couplings  $A_C^q$  ( $q = u, d$ ).

The two-loop gluino contributions originate from the two-loop self energy diagrams (FIG. 2). The corresponding triangle diagrams are obtained by attaching an external gluon or photon line to the self-energy diagrams in all possible ways. In those two-loop diagrams, there are no new suppression factors except the loop integration factor in the corresponding amplitude, and the resulting Wilson coefficients of those dipole moment operators do not involve ultra-violet divergence. Furthermore, there is a parameter space where the two-loop results are comparable with those one-loop contributions because the dependence of the two-loop results on the relevant  $CP$  phases differs from that the one-loop results on the corresponding  $CP$  phases. The contributions of the two-loop gluino-gluino diagrams to the quark EDMs and CEDMs are formulated as

$$\begin{aligned} d_{\tilde{g}(2)}^\gamma &= \frac{8e_q e \alpha_s^2 |m_{\tilde{g}}|}{9(4\pi)^2 m_w^2} F_1(x_q, x_{\tilde{q}_j}, x_{\tilde{g}}, x_{\tilde{g}}, x_{\tilde{q}_i}) \mathbf{Im} \left( (\mathcal{Z}_{\tilde{q}})_{2,j} (\mathcal{Z}_{\tilde{q}}^\dagger)_{j,1} e^{-i\theta_3} \right), \\ d_{\tilde{g}(2)}^g &= \frac{8g_3 \alpha_s^2 |m_{\tilde{g}}|}{9(4\pi)^2 m_w^2} F_3(x_q, x_{\tilde{q}_j}, x_{\tilde{g}}, x_{\tilde{g}}, x_{\tilde{q}_i}) \mathbf{Im} \left( (\mathcal{Z}_{\tilde{q}})_{2,j} (\mathcal{Z}_{\tilde{q}}^\dagger)_{j,1} e^{-i\theta_3} \right), \end{aligned} \quad (9)$$

where  $x_i = m_i^2/m_w^2$ , and the function  $F_i(x_0, x_1, x_2, x_3, x_4)$  ( $i = 1, 3$ ) are defined in Ref.[13].

The contributions of the two loop neutralino-gluino to the quark EDM and CEDM are

given by

$$\begin{aligned}
d_{\chi_k^0(2)}^\gamma &= \frac{4e_q e \alpha \alpha_s}{3(4\pi)^2 s_w^2 c_w^2 m_w^2} \left\{ |m_{\tilde{g}}| F_1(x_q, x_{\tilde{q}_j}, x_{\tilde{g}}, x_{\chi_k^0}, x_{\tilde{q}_i}) \left[ \text{Im} \left( (A_N^q)_{kj} (\mathcal{Z}_{\tilde{q}}^\dagger)_{j,1} \right. \right. \right. \\
&\quad \times (B_N^q)_{ki} (\mathcal{Z}_{\tilde{q}}^\dagger)_{i,1} e^{-i\theta_3} \Big) - \text{Im} \left( (B_N^q)_{kj} (\mathcal{Z}_{\tilde{q}}^\dagger)_{j,2} (A_N^q)_{ki} (\mathcal{Z}_{\tilde{q}}^\dagger)_{i,2} e^{i\theta_3} \right) \Big] \\
&\quad - m_{\chi_k^0} F_2(x_q, x_{\tilde{q}_j}, x_{\tilde{g}}, x_{\chi_k^0}, x_{\tilde{q}_i}) \left[ \text{Im} \left( (A_N^q)_{kj} (\mathcal{Z}_{\tilde{q}}^\dagger)_{j,2} (A_N^q)_{ki} (\mathcal{Z}_{\tilde{q}}^\dagger)_{i,1} \right) \right. \\
&\quad \left. \left. - \text{Im} \left( (B_N^q)_{kj} (\mathcal{Z}_{\tilde{q}}^\dagger)_{j,1} (B_N^q)_{ki} (\mathcal{Z}_{\tilde{q}}^\dagger)_{i,2} \right) \right] \right\}, \\
d_{\chi_k^0(2)}^g &= \frac{4g_3 \alpha \alpha_s}{3(4\pi)^2 s_w^2 c_w^2 m_w^2} \left\{ |m_{\tilde{g}}| F_4(x_q, x_{\tilde{q}_j}, x_{\tilde{g}}, x_{\chi_k^0}, x_{\tilde{q}_i}) \left[ \text{Im} \left( (A_N^q)_{kj} (\mathcal{Z}_{\tilde{q}}^\dagger)_{j,1} \right. \right. \right. \\
&\quad \times (B_N^q)_{ki} (\mathcal{Z}_{\tilde{q}}^\dagger)_{i,1} e^{-i\theta_3} \Big) - \text{Im} \left( (B_N^q)_{kj} (\mathcal{Z}_{\tilde{q}}^\dagger)_{j,2} (A_N^q)_{ki} (\mathcal{Z}_{\tilde{q}}^\dagger)_{i,2} e^{i\theta_3} \right) \Big] \\
&\quad - m_{\chi_k^0} F_5(x_q, x_{\tilde{q}_j}, x_{\tilde{g}}, x_{\chi_k^0}, x_{\tilde{q}_i}) \left[ \text{Im} \left( (A_N^q)_{kj} (\mathcal{Z}_{\tilde{q}}^\dagger)_{j,2} (A_N^q)_{ki} (\mathcal{Z}_{\tilde{q}}^\dagger)_{i,1} \right) \right. \\
&\quad \left. \left. - \text{Im} \left( (B_N^q)_{kj} (\mathcal{Z}_{\tilde{q}}^\dagger)_{j,1} (B_N^q)_{ki} (\mathcal{Z}_{\tilde{q}}^\dagger)_{i,2} \right) \right] \right\}. \tag{10}
\end{aligned}$$

As for the two-loop gluino-chargino contributions to the c-quark EDM and CEDM, we have

$$\begin{aligned}
d_{\chi_k^\pm(2)}^\gamma &= \frac{4e \alpha \alpha_s}{3(4\pi)^2 s_w^2 m_w^2} V_{qQ}^\dagger V_{Qq} \left\{ |m_{\tilde{g}}| F_6(x_Q, x_{\tilde{Q}_j}, x_{\tilde{g}}, x_{\chi_k^\pm}, x_{\tilde{q}_i}) \left[ \text{Im} \left( (A_C^Q)_{kj} (\mathcal{Z}_{\tilde{Q}}^\dagger)_{j,1} \right. \right. \right. \\
&\quad \times (B_C^Q)_{ki} (\mathcal{Z}_{\tilde{Q}}^\dagger)_{i,1} e^{-i\theta_3} \Big) - \text{Im} \left( (B_C^Q)_{kj} (\mathcal{Z}_{\tilde{Q}}^\dagger)_{j,2} (A_C^Q)_{ki} (\mathcal{Z}_{\tilde{Q}}^\dagger)_{i,2} e^{i\theta_3} \right) \Big] \\
&\quad - m_{\chi_k^\pm} F_7(x_Q, x_{\tilde{Q}_j}, x_{\tilde{g}}, x_{\chi_k^\pm}, x_{\tilde{q}_i}) \left[ \text{Im} \left( (A_C^Q)_{kj} (\mathcal{Z}_{\tilde{Q}}^\dagger)_{j,2} (A_C^Q)_{ki} (\mathcal{Z}_{\tilde{Q}}^\dagger)_{i,1} \right) \right. \\
&\quad \left. \left. - \text{Im} \left( (B_C^Q)_{kj} (\mathcal{Z}_{\tilde{Q}}^\dagger)_{j,1} (B_C^Q)_{ki} (\mathcal{Z}_{\tilde{Q}}^\dagger)_{i,2} \right) \right] \right\}, \\
d_{\chi_k^\pm(2)}^g &= \frac{4g_3 \alpha \alpha_s}{3(4\pi)^2 s_w^2 m_w^2} V_{qQ}^\dagger V_{Qq} \left\{ |m_{\tilde{g}}| F_4(x_Q, x_{\tilde{Q}_j}, x_{\tilde{g}}, x_{\chi_k^\pm}, x_{\tilde{q}_i}) \left[ \text{Im} \left( (A_C^Q)_{kj} (\mathcal{Z}_{\tilde{Q}}^\dagger)_{j,1} \right. \right. \right. \\
&\quad \times (B_C^Q)_{ki} (\mathcal{Z}_{\tilde{Q}}^\dagger)_{i,1} e^{-i\theta_3} \Big) - \text{Im} \left( (B_C^Q)_{kj} (\mathcal{Z}_{\tilde{Q}}^\dagger)_{j,2} (A_C^Q)_{ki} (\mathcal{Z}_{\tilde{Q}}^\dagger)_{i,2} e^{i\theta_3} \right) \Big] \\
&\quad - m_{\chi_k^\pm} F_5(x_Q, x_{\tilde{Q}_j}, x_{\tilde{g}}, x_{\chi_k^\pm}, x_{\tilde{q}_i}) \left[ \text{Im} \left( (A_C^Q)_{kj} (\mathcal{Z}_{\tilde{Q}}^\dagger)_{j,2} (A_C^Q)_{ki} (\mathcal{Z}_{\tilde{Q}}^\dagger)_{i,1} \right) \right. \\
&\quad \left. \left. - \text{Im} \left( (B_C^Q)_{kj} (\mathcal{Z}_{\tilde{Q}}^\dagger)_{j,1} (B_C^Q)_{ki} (\mathcal{Z}_{\tilde{Q}}^\dagger)_{i,2} \right) \right] \right\}. \tag{11}
\end{aligned}$$

Note that the last terms of the  $d_{\chi_k^\pm(2)}^\gamma$  and  $d_{\chi_k^\pm(2)}^g$  are not proportional to the suppression factor  $m_q/m_w$ . This implies that the two-loop gluino-chargino diagrams may be the dominant part of the chargino contributions to the quark EDMs and CEDMs.

In order to account for resummation of the logarithmic corrections, we should evolve the coefficients in the quark EDM and CEDM operators at the matching scale  $\mu$  down to



the charm quark mass scale  $m_c \simeq 1.2 \text{ GeV}$  [14] using the renormalization group equations (RGEs)

$$\begin{aligned} d_q^\gamma(\Lambda_\chi) &= \eta_\gamma d_q^\gamma(\mu) , \\ d_q^g(\Lambda_\chi) &= \eta_g d_q^g(\mu) , \end{aligned} \tag{12}$$

where  $\eta_\gamma \simeq 1.53$  and  $\eta_g \simeq 3.4$ . At the low energy scale, we need to include the contributions from the quark CEDMs to the quark EDMs, when we evaluate the numerical value of the charm quark EDM. This is realized by a naive dimensional analysis [15] as

$$d_c = d_c^\gamma + \frac{e}{4\pi} d_c^g . \tag{13}$$

### III. NUMERICAL RESULT

#### A. In case of no flavor mixing

In this subsection we present our numerical results where no flavor mixing is introduced in the squark sector. At present, the upper bound on the neutron EDM is  $d_n \leq 1.1 \times 10^{-25} e \cdot cm$ . In order to make  $d_n$  consistent with this constraint, we take the squark masses of the first generation as  $m_{\tilde{Q}_1} = m_{\tilde{U}_1} = m_{\tilde{D}_1} = 20 \text{ TeV}$ , the  $CP$  phase of the  $\mu$  parameter  $\theta_\mu = 0$ . Without losing generality, we choose the absolute values of the  $\mu$  parameter and soft trilinear quark couplings as  $|\mu| = \mathbf{A}_q = 300 \text{ GeV}$  with  $q = u, d, \dots, t$ , and the soft  $SU(2) \times U(1)$  gaugino masses as  $|m_1| = |m_2| = 600 \text{ GeV}$ . For the soft masses of the third generation squarks, we set  $m_{\tilde{Q}_3} = m_{\tilde{U}_3} = m_{\tilde{D}_3} = 500 \text{ GeV}$ .

Taking  $\tan \beta = 2$ ,  $\arg(\mathbf{A}_q) = 0$ , the  $SU(3)$  gaugino mass  $|m_{\tilde{g}}| = 400 \text{ GeV}$  and the soft masses of the second generation squarks as  $m_{\tilde{Q}_2} = m_{\tilde{U}_2} = m_{\tilde{D}_2} = 300 \text{ GeV}$ , we plot the c-quark EDM  $d_c$  versus the  $CP$  phase of  $m_{\tilde{g}}$  in FIG. 3. With our choice of the parameter space, the c-quark EDM  $d_c$  can reach  $0.5 \times 10^{-20} e \cdot cm$  while the neutron EDM  $d_n$  is below the experimental limit. Numerically, we find that the dominant contributions to  $d_c$  originate from the gluino-squark sector (including the one- and two-loop contributions). The sum of the chargino-squark one-loop and chargino-gluino-squark two-loop contributions to  $d_c$  is less than  $10^{-24} e \cdot cm$ . Through the CKM mechanism, the contributions to  $d_n$  from the second squarks (including squark-chargino one loop and squark-chargino-gluino two-loop diagrams)

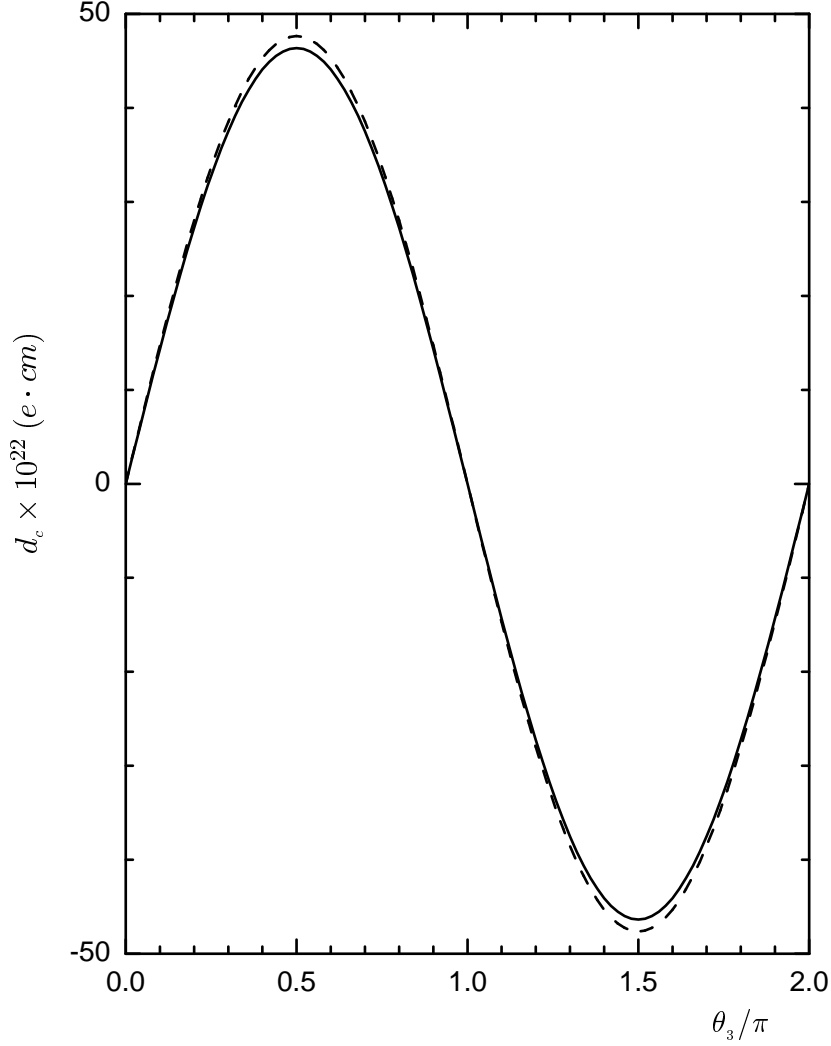


FIG. 3: The c-quark EDM varies with the  $CP$  phase of  $m_{\tilde{g}}$  at  $\tan\beta = 2$ , where the dashed line is the result at the one-loop order, and the solid line is the result at the two-loop order. The other parameters are taken as shown in text.

is below  $10^{-26} e \cdot cm$ . This fact can help us understanding why  $d_n$  satisfies the experimental bound, while  $d_c$  can reach a relatively large value. The choice of the parameter space in FIG. 4 is the same as that in FIG. 3 except for  $\tan\beta = 20$ . Comparing with FIG. 3, the maximum of  $d_c$  in FIG. 3 is about  $0.9 \times 10^{-20} e \cdot cm$ . Since the dependence of gluino-squark two-loop contributions to the quark EDMs on the  $CP$  phases is the same as that of gluino-squark one-loop contributions to the quark EDMs on the  $CP$  phases, the gluino-squark two-loop contributions to  $d_c$  is below 10% with our choice of the parameter space.

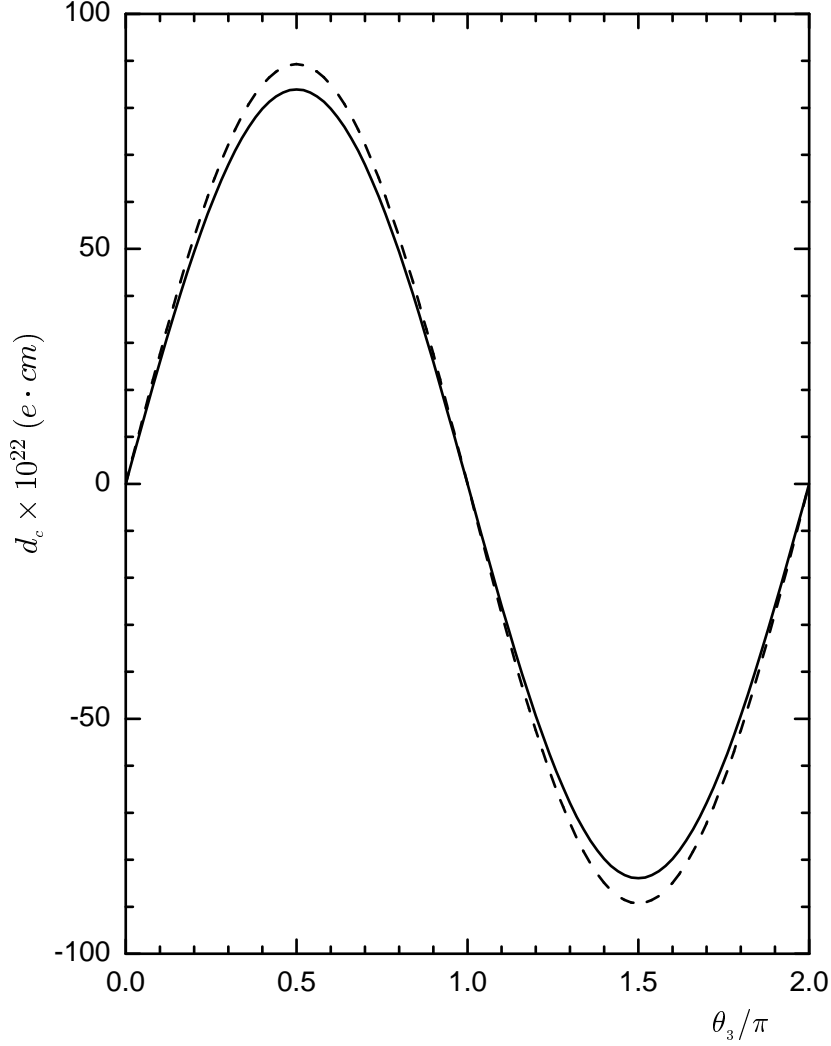


FIG. 4: The c-quark EDM varies with the  $CP$  phase of  $m_{\tilde{g}}$  at  $\tan\beta = 20$ , where the dashed line is the result at the one-loop order, and the solid line is the result at the two-loop order. The other parameters are taken as in text.

Now, we investigate how  $d_c$  varies with the  $CP$  phases of the soft squark Yukawa couplings. Taking  $\tan\beta = 2$ ,  $\arg(m_{\tilde{g}}) = 0$ , we plot  $d_c$  versus the  $CP$  phases  $\arg(\mathbf{A}_c) = \arg(\mathbf{A}_s)$  in FIG. 5, where the other parameters are the same as in FIG. 3. It is clear that the maximum of the absolute value of  $d_c$  is about  $0.9 \times 10^{-20} e \cdot cm$ . With the same choice of the parameter space as for FIG. 5 except  $\tan\beta = 20$ ,  $d_c$  can reach  $5 \times 10^{20} e \cdot cm$ . Nevertheless, the chargino sector which induces a contribution to  $d_n$  is above the experimental upper limit. In order to suppress the chargino contributions to  $d_n$ , we choose  $m_{\tilde{Q}_2} = m_{\tilde{U}_2} = m_{\tilde{D}_2} = 500$  GeV.

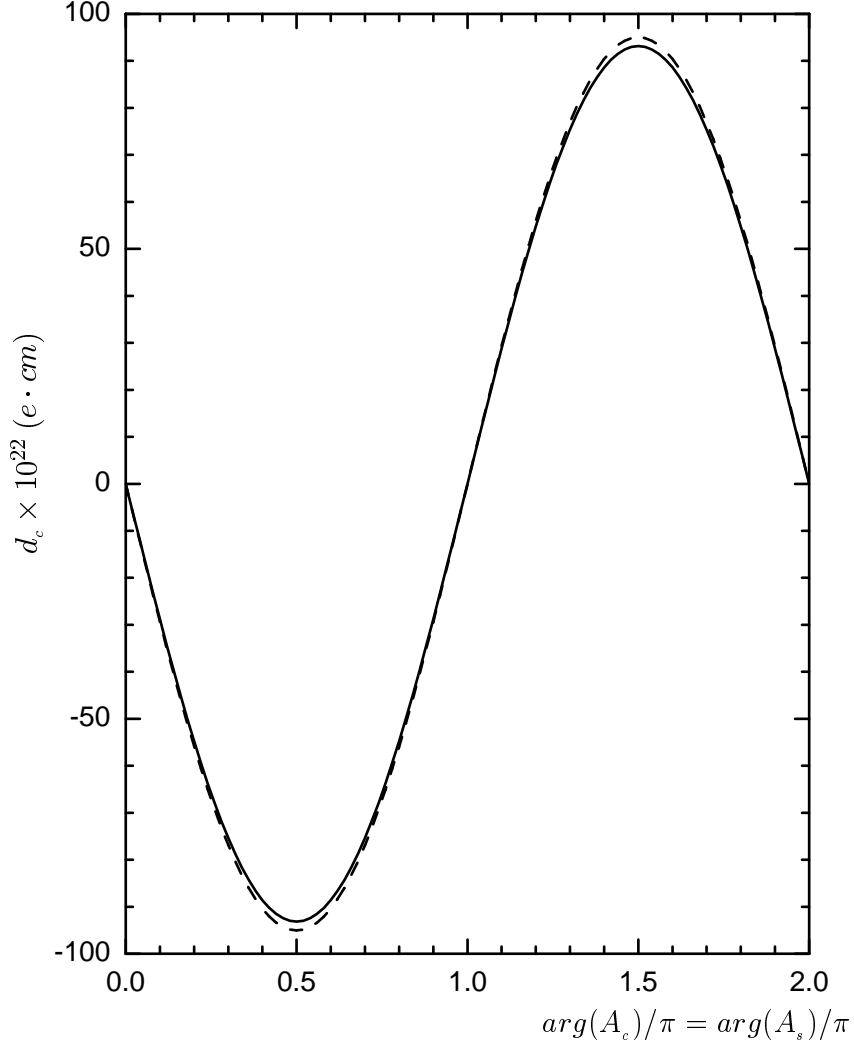


FIG. 5: The c-quark EDM varies with the  $CP$  phases of soft squark Yukawa couplings  $arg(\mathbf{A}_c) = arg(\mathbf{A}_s)$  at  $\tan\beta = 2$ , where the dashed line is the result at one-loop order, and the solid line is the result at two-loop order. The other parameters are taken as in text.

Correspondingly, we set the  $SU(3)$  gaugino mass as  $|m_{\tilde{g}}| = 600$  GeV. Within this scenario, the two-loop gluino-squark contributions are much less than that of one-loop gluino-squark contributions (FIG. 6).

In a similar way, we can investigate how  $d_c$  varies with the  $CP$  phases of the  $SU(2) \times U(1)$  gaugino masses. However, the contributions from the phases of the  $SU(2) \times U(1)$  gaugino masses to  $d_c$  are below  $10^{-23} e \cdot cm$  for our choice of the parameter space.

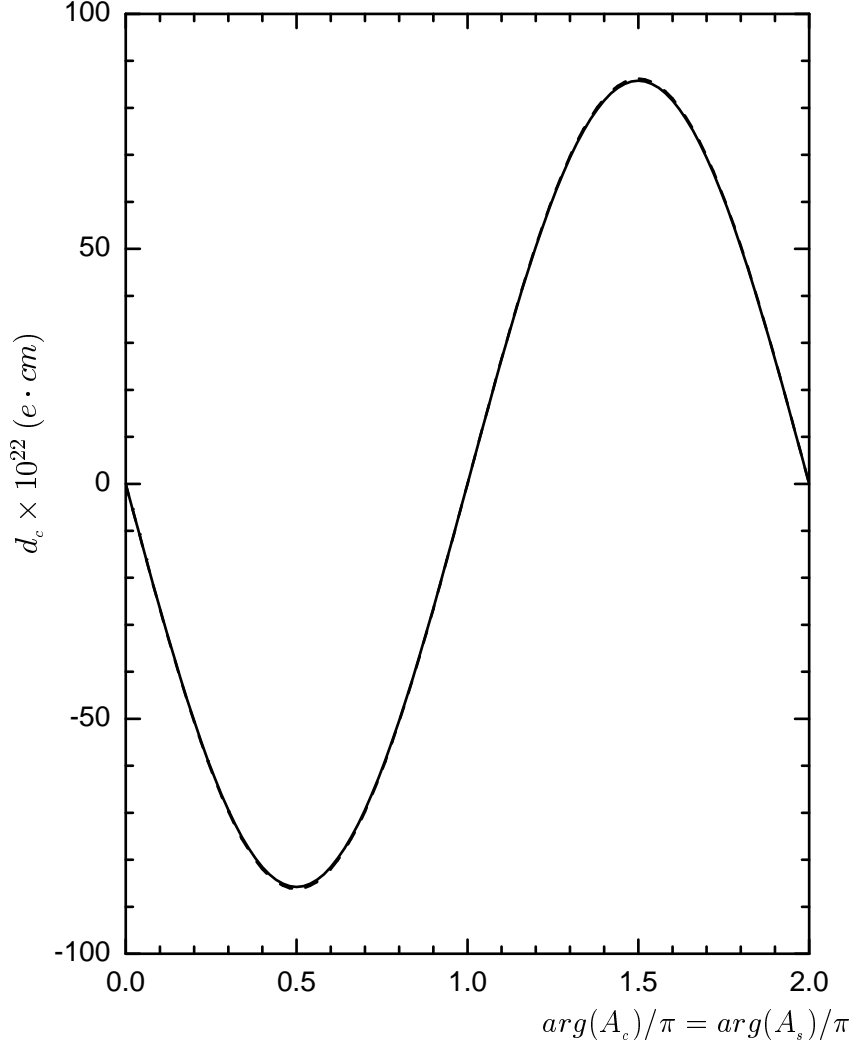


FIG. 6: The c-quark EDM varies with the  $CP$  phases of soft squark Yukawa couplings  $arg(\mathbf{A}_c) = arg(\mathbf{A}_s)$  at  $\tan\beta = 20$ , where the dashed line is the result at one-loop order, and the solid line is the result at two-loop order. The other parameters are taken as in text.

## B. Effective SUSY

In this subsection, we consider the case of the effective SUSY scenario including mixing between the second and the third generation squark. We fix the soft squark masses of the first two generations as heavy as  $20TeV$ . We denote the different left-handed and right-handed squark masses as  $m_{\tilde{L}(\tilde{R})_{1,2,3}}$  respectively and parameterize the the general form of

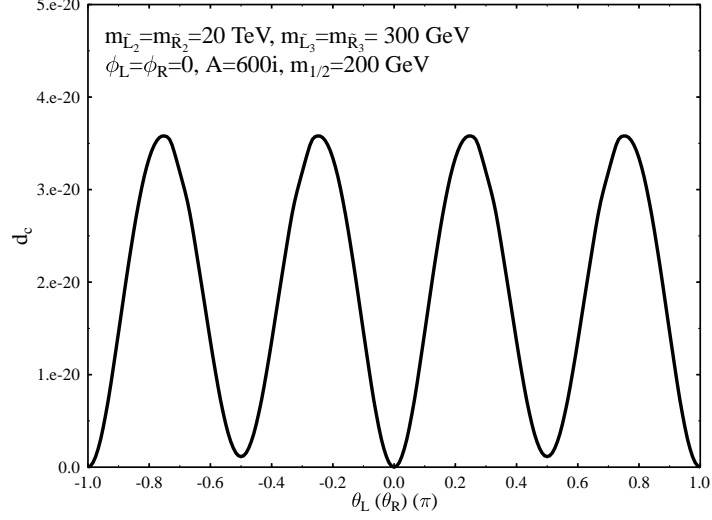


FIG. 7:  $d_c$  as a function of  $\theta_L = \theta_R$  with  $\tan\beta = 5$ ,  $\mu = 150\text{GeV}$ ,  $m_{\tilde{L}_2} = m_{\tilde{R}_2} = 20\text{TeV}$ ,  $m_{\tilde{L}_3} = m_{\tilde{R}_3} = 300\text{GeV}$ ,  $m_{1/2} = 200\text{GeV}$ ,  $A = 600i\text{GeV}$ ,  $m_{\tilde{g}} = 250\text{GeV}$  and  $\phi_L = \phi_R = 0$ .

the soft breaking mass matrix as

$$m_{\tilde{Q}_{L,R}}^2 = Z_{L,R} m_{\tilde{L},\tilde{R}}^2 Z_{L,R}^\dagger, \quad (14)$$

with

$$Z_L = \begin{pmatrix} 1 & & \\ & \cos\theta_L & \sin\theta_L e^{i\phi_L/2} \\ & -\sin\theta_L e^{-i\phi_L/2} & \cos\theta_L \end{pmatrix}, \quad \text{and} \quad m_{\tilde{L}}^2 = \begin{pmatrix} m_{\tilde{L}_1}^2 & & \\ & m_{\tilde{L}_2}^2 & \\ & & m_{\tilde{L}_3}^2 \end{pmatrix}, \quad (15)$$

and the form for the right-handed sector is similar. The free parameters are now  $\tan\beta$ ,  $m_{\tilde{L}_3}$ ,  $m_{\tilde{R}_3}$ ,  $\theta_{L,R}$ ,  $\phi_{L,R}$ , and  $A = |A|e^{i\phi_A}$  for the squark sector;  $\mu = |\mu|e^{i\phi_\mu}$  and  $m_{1/2}$  for the chargino and neutralino sector; and the gluino mass  $m_{\tilde{g}}$ . Assuming the gaugino masses are universal at the GUT scale, the phases of the gaugino masses can be rotated away. Compared with the regular cases, the effective SUSY scenario has four additional parameters:  $\theta_{L,R}$ ,  $\phi_{L,R}$ .

By our calculation, we are convinced that the dominant contribution to  $d_c$  comes from exchange of gluino. Therefore the parameters related to the down squark sector and the chargino and neutralino sector do not affect the numerical result significantly. This fact helps us to reduce the parameter space. We always take the same value of  $m_{\tilde{L}_i}$ ,  $\theta_{L,R}$  and  $\phi_{L,R}$  for the up and down squark sector. We set  $\tan\beta = 5$  and  $\mu = 150\text{GeV}$  in our calculations.

By the above discussions we are left with only 8 free parameters:  $m_{\tilde{L}_3}(=m_{\tilde{R}_3})$ ,  $\theta_{L,R}$ ,  $\phi_{L,R}$ , and  $A = |A|e^{i\phi_A}$ . We first show the effects of the mixing angle  $\theta_{L,R}$  in Fig. 7. We notice

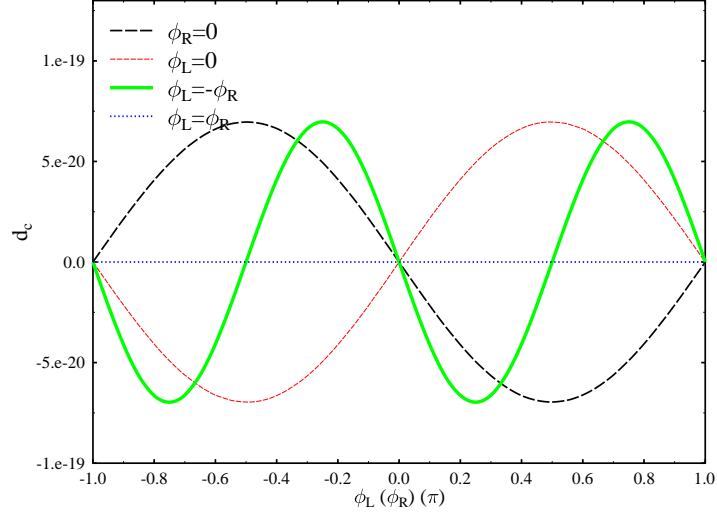


FIG. 8:  $d_c$  as a function of  $\theta_L$  (long dashed line),  $\theta_R$  (short dashed line),  $\theta_L = -\theta_R$  (solid line) and  $\theta_L = \theta_R$  (dotted line) for  $\theta_L = \theta_R = \pi/4$ . Other parameters are the same as those in Fig. 7.

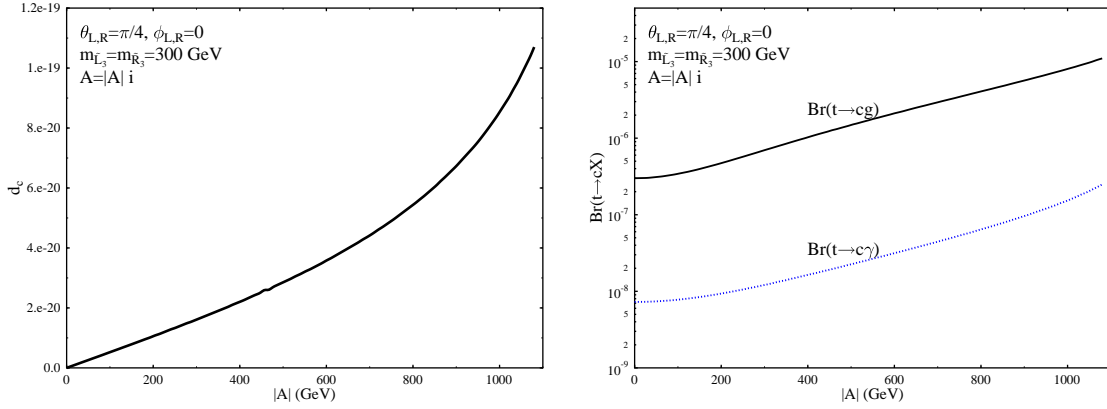


FIG. 9:  $d_c$  (left panel) and the branching ratio of  $t \rightarrow c\gamma$  (right panel) as functions of  $|A|$  for maximal mixing angle  $\theta_L = \theta_R = \pi/4$  and  $\phi_{L,R} = 0$ . Other parameters are the same as those in Fig. 7.

that if the mixing angle is zero,  $d_c$  is nearly zero, which is a direct result of extremely heavy charm squark of about  $20TeV$ . For maximal mixing,  $\theta_{L,R} = \pi/4$ , we get the maximal  $d_c$ .

The contribution to  $d_c$  from the phases of  $\phi_{L,R}$  is plotted in Fig. 8 for maximal mixing angle  $\theta_L = \theta_R = \pi/4$ . It is interesting to notice that when  $\theta_L = \theta_R$  (dotted line) the contributions from  $\phi_L$  and  $\phi_R$  cancel each other.

The dependence of  $d_c$  on the magnitude of  $A$  is plotted in Fig. 9 (on the left panel). For

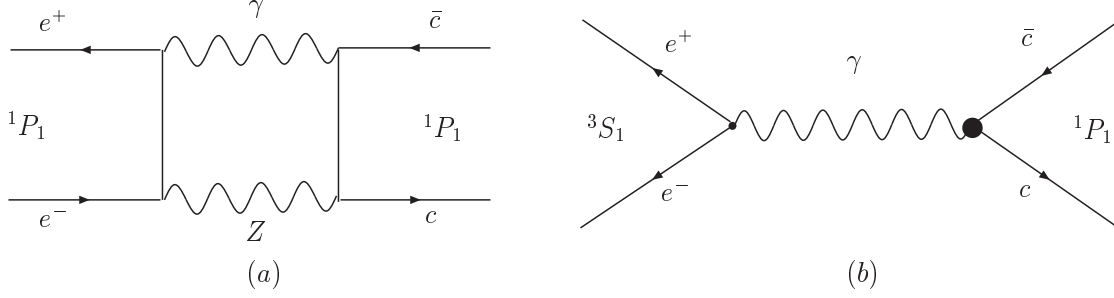


FIG. 10: The Feynman diagrams for production of the  $^1P_1$  charmonium resonance in  $e^+e^-$  scattering from (a) the CP-conserving and (b) CP-violating modes. The dark blob stands for insertion of the effective operator (1).

large  $|A|$ , not only the CP violation is enhanced, but also the effects of the lighter stop mass is suppressed. Therefore  $d_c$  increases rapidly with increasing value of  $|A|$ . The maximal value of  $d_c$  can reach about  $\sim 10^{-19} e \cdot cm$ .

The numerical results show that in the effective SUSY scenario, where all the bounds set by the low energy experiments are satisfied, the EDM of charm quark can be enhanced by an order of magnitude due to the large mixing between the second and third generations of up squark.

Finally, we show the flavor changing effects of large mixing between scharm and stop. The branching ratios of  $t \rightarrow c\gamma$  and  $t \rightarrow cg$  induced by the mixing are plotted on the right panel of Fig. 9, which are below  $\sim 10^{-5}$  and  $\sim 10^{-7}$  respectively. We have adopted the LoopTools package[21] to finish the loop integrations. In fact, the present experiments do not constrain the mixing between scharm and stop[22].

#### IV. $h_c$ PRODUCTION IN $e^+e^-$ COLLIDER

Recently the E835 Collaboration at Fermilab[23] and the CLEO Collaboration[24] have announced the observation of the  $^1P_1$  CP-odd state  $h_c$ . However, the direct production of the  $^1P_1$  charmonium resonance at the  $e^+e^-$  annihilation plays an important role in probing the charm quark EDM, since the coupling of photon to the  $^1P_1$  charmonium, as shown in Fig. 10 (b), is identical to the effective operator in Eq. (1). The coupling of the current



density[25]

$$J_\mu(\bar{c}c|{}^1P_1) = \bar{c}(x)\overleftrightarrow{\partial}_\mu\gamma_5c(x) \quad (16)$$

to a photon results in the effective operator (1). We can also check the quantum numbers of the process in Fig. 10 (b). Transition from the initial  ${}^3S_1$  ( $J^{PC} = 1^{--}$ ) state to the final  ${}^1P_1$  ( $J^{PC} = 1^{+-}$ ) state requires the photon-charm-charm vertex, denoted as dark blob in Fig. 10 (b), to be  $-$  or  $+$  under P and C transformations. We find that the operator (1) just satisfies the requirement. Under P and C transformations we have

$$A_\mu \xrightarrow{P} A^\mu, \quad A_\mu \xrightarrow{C} -A_\mu, \quad (17)$$

$$\sigma_{\mu\nu}\gamma_5q^\nu \xrightarrow{P} -\sigma^{\mu\nu}\gamma_5q_\nu, \quad \sigma_{\mu\nu}\gamma_5q^\nu \xrightarrow{C} -\sigma_{\mu\nu}\gamma_5q^\nu. \quad (18)$$

The operator (1) obviously possesses right quantum numbers.

In the SM, the  $h_c$  ( ${}^1P_1$ ) meson can be produced via  $\gamma Z$  and  $ZZ$  box diagrams, as shown in Fig. 10 (a), which are CP-conserving processes. As shown in Ref. [17, 18], the effective Hamiltonian is given as

$$H_{SM} = \frac{\alpha}{3\pi\sqrt{2}}G_Fm_em_c\mathfrak{B}J_\mu(\bar{c}c|{}^1P_1) \cdot J^\mu(e^+e^-|{}^1P_1), \quad (19)$$

where the current  $J_\mu$  is defined in Eq. (16) and  $\mathfrak{B}$  is a standard loop integral. In the minimal SUSY, there is another diagram where  $Z$  is replaced by a CP-odd Higgs  $A^0$ , and generally it is considered to be smaller than the SM contribution[17].

The effective Hamiltonian responsible for the CP-violating process of  $h_c$  production via the charm quark EDM, shown in Fig. 10 (b), is given as

$$H_{SUSY} = \frac{4\pi\alpha}{M_{h_c}^2}\frac{d_c}{e}J_\mu(\bar{c}c|{}^1P_1) \cdot J^\mu(e^+e^-|{}^3S_1), \quad (20)$$

where  $J^\mu(e^+e^-|{}^3S_1) = \bar{e}\gamma^\mu e$ . Comparing the two contributions we obtain the production amplitude of  $h_c$  via the CP-violating process and it can overtake the CP-conserving one if the EDM of the charm quark exceeds the critical value[17]

$$\left|\frac{d_c^{crit}}{e}\right| \sim \frac{G_Fm_e}{12\sqrt{2}\pi^2}\frac{M_{h_c}^2}{M_Z^2}\log\frac{m_c}{m_e} \sim 10^{-26}cm. \quad (21)$$

The numerical results presented in last section show that the EDM of the charm quark in the effective SUSY is well above the critical value  $10^{-26}e \cdot cm$ . Therefore, direct production of  $h_c$  at  $e^+e^-$  annihilation is expected to be closely related to the EDM of the charm quark or even determined by it.

Assuming that the center-of-mass energy of BEPC or CLEO-C is set at the vicinity of  $M_{h_c}(\sim 3524\text{MeV})$ [24], we get the cross section for  $h_c$  production as [17, 18]

$$\sigma(e^+e^- \rightarrow h_c) = 27 \left| \frac{d_c}{e} \right|^2 \left| \frac{R'_P(0)}{R_S(0)} \right|^2 \sigma(e^+e^- \rightarrow {}^3S_1) \sim 27 \left| \frac{M_{h_c} d_c}{e} \right|^2 \sigma(e^+e^- \rightarrow {}^3S_1) , \quad (22)$$

where  $R_P$  and  $R_S$  are the wave functions of  $h_c$  and  ${}^3S_1$  states, respectively. The smallness of the EDM of charm quark predicts a very small  $h_c$  production rate, which is about 10 orders of magnitude smaller than  $\sigma(e^+e^- \rightarrow {}^3S_1)$  for  $h_c \sim 10^{-20} e \cdot \text{cm}$ . With the upgraded BEPC[19] and CLEO-C programs[20], a data sample of  $10^9 \sim 10^{10} J/\psi$  will be collected. We can estimate the number of  $h_c$  events as[17]

$$N_{h_c} \sim 27 \times N_{J/\psi} \left| \frac{M_{h_c} d_c}{e} \right|^2 \sim 10^{-10} \left| \frac{d_c/e}{10^{-20} \text{cm}} \right|^2 \times N_{J/\psi} , \quad (23)$$

which predicts maximally  $10^2 \sim 10^3$   $h_c$  events per year in the effective SUSY scenario with the upgraded BEPC and CLEO-C luminosity. With the high energy resolution detector at BES-III[26], the spectrum of gamma at the inclusive channel  $h_c \rightarrow \gamma \eta_c$  can be well determined with high efficiency. The directly produced  $h_c$  may be in the observable range at BES-III[27].

## V. CONCLUSION

Considering the neutron EDM constraint, we investigate the EDM of charm quark in the  $CP$  violating MSSM. Typically,  $d_c$  can reach about  $10^{-20} e \cdot \text{cm}$  as we include the contributions from c-quark CEDM. The mixing between the second and third generation squarks in the effective SUSY scenario further enhances  $d_c$  to about  $10^{-19} e \cdot \text{cm}$ .

Large EDM of charm quark can induce a direct production of the  $1^1P_1$  CP-odd state charmonium,  $h_c$ , via a CP-violating process at  $e^+e^-$  annihilation. By the luminosity and efficiency of the upgraded BEPC-II or CLEO-C (with  $10^{10} J/\psi$  collected) if no  $h_c$  is observed, a rigorous constraint on the charm quark EDM would be set, as  $d_c \lesssim 10^{-19} e \cdot \text{cm}$ . On the contrary, any signal of  $h_c$  production will indicate large EDM of the charm quark and becomes a clear evidence of new physics beyond the SM.

The BEPC-II and CLEO-C will provide excellent opportunities to probe many important theoretical objects. Among them, the charm quark EDM is a prominent one because it is a clear signal of CP violation and an evidence for new physics beyond the SM[28]. Our

numerical results indicate that the direct production rate of  $h_c$  at the vicinity of  $M_{h_c} \sim 3524 \text{ MeV}$  [24] may be dominated by the charm quark EDM as long as new physics such as the MSSM is involved. Observation of  $h_c$  thus produced would clearly indicate new physics beyond the SM, conversely, a negative result would set a rigorous constraint to the parameter space for the new physics. Therefore we are looking forward to the new data of BEPC-II and CLEO-C to help us gaining insight to the new physics beyond the SM.

### Acknowledgments

We thank X.Y. Shen and C.Z.Yuan for helpful discussions. This work is supported in part by the National Natural Science Foundation of China under the Grand No. 10105004, 10120130794, 19925523, 10047004, 10475042, 90303004, the Ministry of Science and Technology of China under Grant NO. NKBRSF G19990754, and the Academy of Finland under the contracts no. 104915 and 107293.

- 
- [1] J. M. Christensen, J. W. Cronin, V. L. Fitch, R. Turlay, Phys. Rev. Lett. **13** (1964) 138.
  - [2] K. Abe, *et al.*, [Belle Collaboration], Phys. Rev. Lett. **87** (2001) 091802; B. Aubert, *et al.*, [BaBar Collaboration], Phys. Rev. Lett. **89** (2002) 201802.
  - [3] A. Pilaftsis, Phys. Lett. B **435**, 88(1998); D. A. Demir, Phys. Rev. D **60**, 055006(1999); A. Pilaftsis and C. E. Wagner, Nucl. Phys. B **553**, 3(1999); T. Ibrahim and P. Nath, Phys. Rev. D **63**, 035009(2001); M. Carena, J. Ellis, A. Pilaftsis, and C. E. Wagner, Nucl. Phys. B **586**, 92(2000); Phys. Lett. B **495**, 155(2000).
  - [4] T. Ibrahim, P. Nath, Phys. Lett. B **418**, 98(1998); Phys. Rev. D **57**, 478(1998); **58**, 111301(1998); **61**, 093004(2000); M. Brhlik, G. J. Good, G. L. Kane, *ibid.* **59**, 115004(1999); A. Bartl, T. Gajdosik, W. Porod, P. Stockinger and H. Stremnitzer, *ibid.* **60**, 073003(1999).
  - [5] P. Nath, Phys. Rev. Lett. **66**, 2565(1991); Y. Kizukuri and N. Oshimo, Phys. Rev. D. **45**, 1806(1992); **46**, 3025(1992); D. Chang, W. Keung and A. Pilaftsis, Phys. Rev. Lett. **82**, 900(1999); A. Pilaftsis, Phys. Lett. B **471**, 174(1999); D. Chang, W. Chang and W. Keung, *ibid.* **478**, 239(2000); T. F. Feng, T. Huang, X. Q. Li, X. M. Zhang, and S. M. Zhao, Phys. Rev. D. **68**, 016004(2003).

- [6] F. Kruger and J. C. Romao, Phys. Rev. D **62**, 034020(2000); T. M. Aliev, D. A. Demir, and M. Savci, *ibid.* **62**, 074016(2000).
- [7] D. A. Demir and M. B. Voloshin, Phys. Rev. D **63**, 115011(2001).
- [8] A. Ali, H. Asatrian, and C. Greub, Phys. Lett. B **429**, 87(1998); A. Ali and E. Lunghi, Eur. Phys. J C **21**, 683(2001); T. Nihei, Prog. Theor. Phys. **98**, 1157(1997); S. Baek and P. Ko, Phys. Rev. Lett. **83**, 488(1999); D. A. Demir, A. Masiero, and O. Vives, *ibid.* **82**, 2447(1999); S. Baek, Phys. Rev. D **67**, 096004(2003); A. Dedes and A. Pilaftsis, *ibid.* **67**, 015012(2003).
- [9] J. Ellis, S. Ferrara and D. V. Nanopoulos, Phys. Lett. **B114** (1982) 231; J. Polchinski and M. B. Wise, Phys. Lett. **B125**(1983) 393; F. del Aguila, M. B. Gavela, J. A. Grifols and A. Mendez, Phys. Lett. **B126** (1983) 71; D. V. Nanopoulos and M. Srednicki, Phys. Lett. **B128** (1983) 61.
- [10] T. Falk and K. A. Olive, Phys. Lett. **B375** (1996) 196; Phys. Lett. **B439** (1998) 71; T. Ibrahim and P. Nath, Phys. Lett. **B418** (1998) 98; Phys. Rev. **D57** (1998) 478; M. Brhlik, G. J. Good and G. L. Kane, Phys. Rev. **D59** (1999) 115004.
- [11] P. Nath, Phys. Rev. Lett. **66** (1991) 2565; Y. Kizukuri and N. Oshimo, Phys. Rev. **D45** (1992) 1806; Phys. Rev. **D46**, 3025 (1992).
- [12] A. I. Davydychev and J. B. Tausk, Nucl. Phys. B. **397**, 123(1993).
- [13] T. -F. Feng, Phys. Rev. D. **70**, 096012(2004) (hep-ph/0405192); T. -F. Feng, X. -Q. Li, J. Maalampi and X. Zhang, hep-ph/0412147.
- [14] R. Arnowitt, J. Lopez, and D. V. Nanopoulos, Phys. Rev. D. **42**, 2423(1990); R. Arnowitt, M. Duff and K. Stelle, *ibid.* **43**, 3085(1991).
- [15] A. Manohar, and H. Georgi, Nucl. Phys. B. **234**, 189(1984).
- [16] M. Dine, A. Kagan and S. Samuel, Phys. Lett. **B243**, 250 (1990) ; S. Dimopoulos and G. F. Giudice, Phys. Lett. **B357**, 573 (1995); A. Pomarol and D. Tommasini, Nucl. Phys. **B466**, 3 (1996); A. G. Cohen, D. B. Kaplan and A. E. Nelson, Phys. Lett. **B388**, 588 (1996); D. E. Kaplan, F. Lepeintre, A. Masiero, A. E. Nelson and A. Riotto, Phys. Rev. D **60**, 055003 (1999); J. Hisano, K. Kurosawa and Y. Nomura, Phys. Lett. **B445**, 316 (1999);
- [17] Z. Z. Aydin, U. Erkarslan, Phys. Rev. D **67** (2003) 036006.
- [18] D. A. Demir, M. B. Voloshin, Phys. Rev. D **63** (2001) 115011.
- [19] Z. Zhao, eConf C010430 (2001) M10.
- [20] L. K. Gibbons, eConf C010430 (2001) T06.

- [21] T. Hahn, M. Perez-Victoria, Comput. Phys. Commun. 118 (1999) 153.
- [22] J.L. Diaz-Cruz, H. J. He, C.-P. Yuan, Phys. Lett. **B 530** (2002) 179; T. Han, K.-i. Hikasa, J. M. Yang, X. Zhang, Phys. Rev. D**70**, 055001 (2004).
- [23] Talk by C. Patrignani at the International Workshop on Heavy Quarkonium, October 12-15, 2004 , IHEP Beijing.
- [24] Talk by A. Tomaradze at the International Workshop on Heavy Quarkonium, October 12-15, 2004 , IHEP Beijing.
- [25] V. A. Novikov, L. B. Okun, M. A. Shifman, A. I. Vainshtein, M. B. Voloshin and V. I. Zakharov, Phys. Rept. **41** (1978) 1.
- [26] Talk by P. Wang and X.Y.Shen at the International Workshop on Heavy Quarkonium, October 12-15, 2004 , IHEP Beijing.
- [27] Y.P. Kuang, Phys. Rev. D **65**, 094024 (2002).
- [28] Xinmin Zhang, "PROBING FOR NEW PHYSICS IN J / PSI DECAYS" hep-ph/0010105; J.P. Ma, R.G. Ping and B.S. Zou, Phys. Lett. **B 580** (2004) 163.